

Image Addition by Computer Generated Multiplexed Holograms

M. Araiza E, G. Miramontes de L., I. de la Rosa V.,
Laboratorio de Procesamiento Digital de Señales,
Universidad Autónoma de Zacateca, Zacatecas, Zac.- 98000.
TEL: +(492) 9239407, ext. 1518 correo-e: araizama@cantera.reduaz.mx

S. Guel S.,
Instituto de Investigación en Comunicación Óptica (IICO),
Universidad Autónoma de San Luis Potosí (UASLP), San Luis Potosí, S.L.P.- 78000.
Tel: +(444) 8250183, correo-e: sguel@cactus.iico.uaslp.mx

y

J. J. Villa H., C. Sifuentes G., E. García D.
Laboratorio de Procesamiento Digital de Señales,
Universidad Autónoma de Zacateca, Zacatecas, Zac.- 98000.
TEL: +(492) 9239407, ext. 1518 correo-e: jvillah@cantera.reduaz.mx

Abstract – Se describe una nueva técnica para realizar suma de imágenes con Hologramas Multiplexados Generados por Computadora (HMGC). El propósito de este trabajo es tratar objetos bidimensionales, que son almacenados en un holograma. Cuando se reconstruyen los hologramas, las imágenes aparecen simultáneamente en la misma dirección y en el mismo orden de difracción, recuperando una imagen más compleja. Los resultados experimentales demuestran el procedimiento propuesto.

Abstract— A new approach to perform image addition via computer generated multiplexed holograms is described. The purpose of this work is to handle flat objects that are to be stored in a hologram. When holograms are reconstructed, images appear simultaneously in the same direction and same diffraction order, thus recovering a more complex image. The experimental results demonstrate the suggested procedure.

Palabras Clave – computer generated hologram, flat object, image addition, multiplexed holograms.

I. INTRODUCTION

THE Computer generated holograms (CGH) have become a branch of modern optics that have called the attention of a large number of researchers and engineers, due to their multiple applications [1]. Conceptually they can be summarized as follows [2] - [4]: the Fourier transform of a discrete flat object (two-dimensional digital image) is performed. The resulting amplitude and phase of each point are coded with the aid of cells, as the one shown in Figure 1, where amplitude and phase are represented respectively by the width and position of a rectangle inside the cell. Performing the above procedure, a discrete interference pattern is generated, which is graphed and later photographically reduced until a transparency of a proper size to diffract light is obtained. When such transparency is illuminated with an expanded coherent wavefront, the image of the original flat object can be reconstructed with the aid of a lens. During the last years, several multiplexing methods have been suggested to codify two or four flat objects simultaneously, which are: the double-multiplexed [5] and the four-channel [6] methods. All these methods have a common characteristic: multiplexed images appear in orthogonal directions. In this work we propose some cell designs, which allow the multiplexing of two or three flat objects (FO) in the same direction and same order. The proposed method carries out an image addition. This work is organized as follows: in section II the codification method and the different cell designs are described. In section III the experimental results are presented, and finally in section IV some concluding remarks are given.

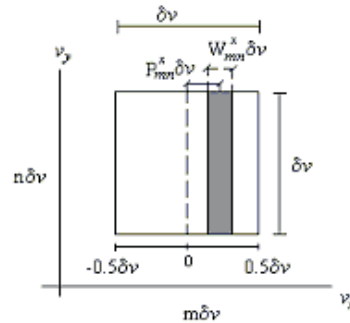


Figure 1. Structure of a (m, n) basic cell for a binary hologram. Parameters W and P codify the amplitude and phase respectively.

II. CODIFICATION TECHNIQUE AND CELL DESIGNS

Figure 2 shows a cell design of size $\delta\nu \times \delta\nu$, with coordinates $(m\delta\nu, n\delta\nu)$ using a couple of rectangles with the purpose of duplicating the amount of information contained in a hologram. This procedure allows codifying up to four free parameters. Each rectangle's width is defined: $W_{mn}^X \delta\nu$ and $W_{mn}^{-X} \delta\nu$, and lateral changes are introduced by variables: $P_{mn}^X \delta\nu$ and $P_{mn}^{-X} \delta\nu$, with constant height. Our purpose is to codify two flat objects: one $u_X(x, y)$, with parameters $W_{mn}^X \delta\nu$ and $P_{mn}^X \delta\nu$, and a second one $u_{-X}(x, y)$, with parameters $W_{mn}^{-X} \delta\nu$ and $P_{mn}^{-X} \delta\nu$. Both images are obtained in the diffraction order ± 1 . The letters $-X$ and X are used to identify different flat objects. The binary transmittance H of the holograms can be written as:

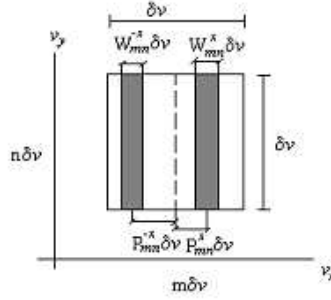


Figure 2. Design of a (m, n) cell to duplicate the amount of information contained in a hologram.

$$H(\nu_x, \nu_y) = \sum_{m,n} \left\{ \text{rect} \left[\frac{\nu_x - m\delta\nu - P_{mn}^X \delta\nu}{W_{mn}^X \delta\nu} \right] \text{rect} \left[\frac{\nu_y - n\delta\nu}{\delta\nu} \right] + \text{rect} \left[\frac{\nu_x - m\delta\nu + P_{mn}^{-X} \delta\nu}{W_{mn}^{-X} \delta\nu} \right] \text{rect} \left[\frac{\nu_y - n\delta\nu}{\delta\nu} \right] \right\}. \quad (1)$$

Each value (m, n) refers to a cell. The rect function is defined only horizontally, as: $\text{rect}(x) = 1$ when $|x| \leq 1/2$ and equal to zero otherwise while in vertical direction the rect function is constant and equal to $\delta\nu$ for all n , so it can be neglected.

At the image plane, the field distribution $h(x, y)$ appears as the inverse Fourier transform (IFT) of $H(\nu_x, \nu_y)$, as:

$$h(x, y) = \int \int H(\nu_x, \nu_y) \exp[2\pi i(x\nu_x + y\nu_y)] d\nu_x d\nu_y = \sum_{m,n} \left\{ (x\delta\nu W_{mn}^X \pi) \text{sinc}(x\delta\nu W_{mn}^X \pi) \exp[2\pi i x(m + P_{mn}^X) \delta\nu] + (x\delta\nu W_{mn}^{-X} \pi) \text{sinc}(x\delta\nu W_{mn}^{-X} \pi) \exp[2\pi i x(m + P_{mn}^{-X}) \delta\nu] \right\}. \quad (2)$$

Where, we have $4N^2$ free parameters $(W_{mn}^X, P_{mn}^X, W_{mn}^{-X}, P_{mn}^{-X})$. Besides, it is desired that the complex amplitude $h(x, y)$ describes the images $u^X(x, y)$ and $u^{-X}(x, y)$. We assume that $u^X(x, y)$ and $u^{-X}(x, y)$ are nonzero inside the rect function area; and that the first diffraction order is along the x direction located at x_0 . Where $u^X(x, y)$ and $u^{-X}(x, y)$ can be expressed in terms of Fourier Transforms (FT), in amplitude and phase as follow:

$$U^X = (m\delta\nu) = A_{mn}^X \exp(i\phi_{mn}^X), \quad (3)$$

$$U^{-X} = (m\delta\nu) = A_{mn}^{-X} \exp(i\phi_{mn}^{-X}). \quad (4)$$

As we can see, $h(x, y)$ is almost a Fourier series except for the sinc function, and the equations $u^X(x - x_0, y)$ and $u^{-X}(x - x_0, y)$ are represented by a Fourier series inside the area (∇x) . Both series can be set equal by matching the corresponding Fourier coefficients one by one. After some approximation we get the 4 parameters:

$$\sin(\pi W_{mn}^X) = A_{mn}^X, \quad (5)$$

$$2\pi P_{mn}^X = \phi_{mn}^X, \tag{6}$$

$$\sin(\pi W_{mn}^{-X}) = A_{mn}^{-X}, \tag{7}$$

$$-2\pi P_{mn}^{-X} = \phi_{mn}^{-X}. \tag{8}$$

The analysis of results above shows that the right term in (8) physically corresponds to the complex conjugate of the object represented by $-X$ rectangle, as we can see:

$$\exp(i\phi_{mn}^{-X}) = \exp(-2\pi i P_{mn}^{-X}) = [\exp(2\pi i P_{mn}^{-X})]^*, \tag{9}$$

where asterisk denotes the complex conjugate. Note, the $-X$ rectangle changes sign when is plotted, because is graphed in left side of cell, therefore the complex conjugate of (9) is neglected, hence we have:

$$P_{mn}^{-X} = \frac{\phi_{mn}^{-X}}{2\pi}. \tag{10}$$

It is understood that a double complex conjugate is executed (in the $-X$ rectangle), which is implicit during the performance of the method, as we will see in the results.

Analysis of results above led to another cell design, with rectangles to the right of origin as shown in Figure 3(a). Mathematical analysis of cell is done under the same codification principle as in cell of Figure 2. For cell in Figure 3(a), the free parameters are identical to (5) - (7), (10), respectively, changing $-X$ by $X1$ and X by $X2$. Therefore, the cells in Figures 2 and 3(a) can be used indistinctly to obtain the same results. Besides, they can be obtained by adding two basic cells (see Figure 1). So that three of these will triple the information contained in the hologram. For this, cell in Figure 3(b) is analyzed and consequently the following free parameters can be summarized as follows:

$$W_{mn}^{X_i} = \frac{\sin^{-1}(A_{mn}^{X_i})}{\pi}, \quad i = 1, 2, 3 \tag{11}$$

$$P_{mn}^{X_i} = \frac{\phi_{mn}^{X_i}}{2\pi}, \tag{12}$$

where i represents the number of FO's to be codified.

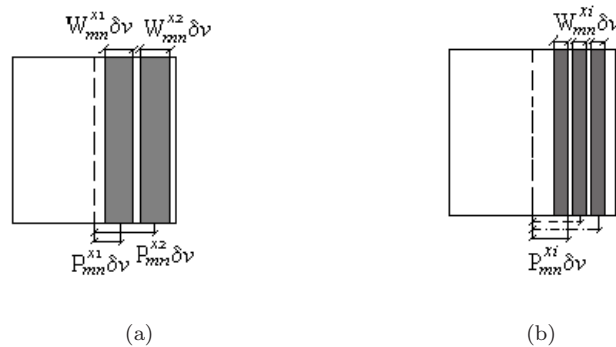


Figure 3. Designs of cells that (a) duplicate and (b) triple the information contained in a hologram.

Therefore, it is evident that the amount of information contained in a CGH can be increased according to basic cells number; but a limit exists due to cell finite size. We can go further away. The results are shown in the next section.

III. RESULTS AND DISCUSSIONS

The following results show the effectiveness of the proposed method. The generated binary holograms were computed with the MatLab software. Besides, we used a plotter HP LaserJet 6M with a 600×600 -dpi spatial resolution. The shape of the FO's is denoted as a draft. The sizes of generated holograms were 128×128 and 200×200 cells. The holograms once plotted, were photographically reduced to obtain a transparency of size between 1.0 or 1.5 cm^2 , respectively, and then they were set in an optical system as that shown in Figure 4. A laser beam is expanded to illuminate the hologram transparency and then focused with aid of a lens. All images together with its conjugate appear at the image plane.

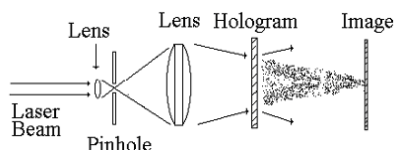


Figure 4. Optical system set up for image reconstruction.

To demonstrate the equivalence between cells in Figures 2 and 3(a), holograms were generated using (5) - (8), and their equivalence, respectively, using the FO's shown in Figure 5(a) and (b). In Figure 5(c) and (d) the reconstructed images are shown. As seen, results are the same. Should be noted in this case, no overlapping among images exists, because drafts of FO's have different locations.

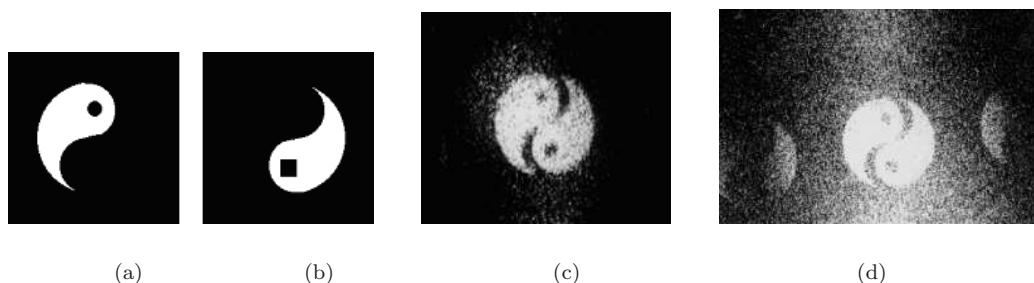


Figure 5. (a) and (b) FO's. (c) and (d) Reconstructed images. Both pictures show same results: (c) is obtained using cell in Figure 2, and (d) using cell in Figure 3(a). Holograms are 200×200 cells.

Now, suppose FO's drafts coincide totally or in parts within their corresponding coordinates, as illustrated in Figure 6(a) and (b). We would expect in this case, the flat reconstructed partial images to overlap as illustrated in Figure 6(c). This overlapping can be avoided cancelling one of the negative signs that are implicit in rectangle $-X$ (see Figure 2). This cancellation could be done in two ways: the minus sign is neglected in (8) or the $-X$ rectangle is plotted to the right side of the cell, as shown in Figure 2. For example: drafts in Figure 6(a) and (b) are the same as in Figure 7(a) and (b) but the last are drawn to the right of the square; as seen in results shown in Figure 7(c).

For triple multiplexing, cell in Figure 3(b) and FO's in Figure 8(a) - (c) were used; while

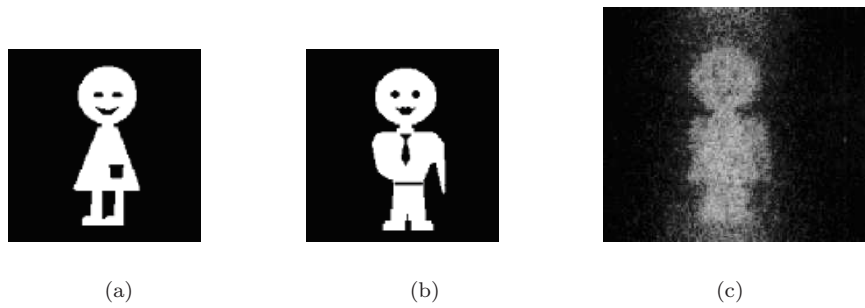


Figure 6. (a) and (b) FO's draft with overlapping coordinates. Picture (c), shows overlapping images.

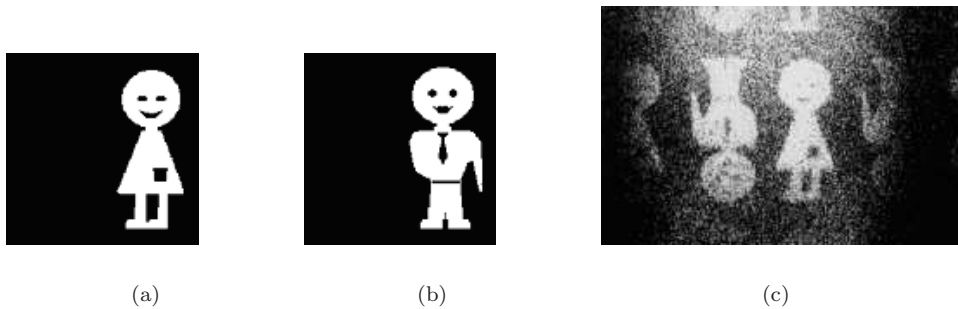


Figure 7. (a) and (b) show FO's with overlapping coordinates. (c) Clearly shows separation of images, when complex conjugate of one of them is obtained during reconstruction.

Figure 8(d) shows the recovered images. As we can see, the resolution decrease when the number codified FO's is increased. Other examples are shown in the following paragraphs.

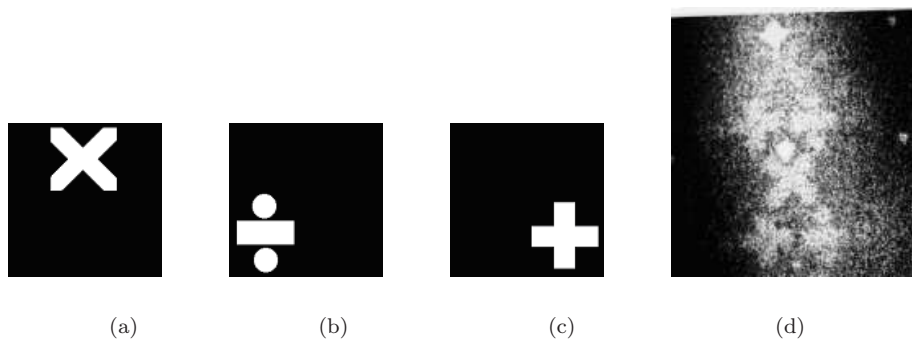


Figure 8. (a) - (c) FO's. (d) Image recuperated using cell in Figure 3(b). Hologram was 200×200 cells.

Figure 9(b) and (c) show identical results; they correspond to FO's in Figure 5(a) and (b). Figure 9(b) was obtained using the cell shown in Figure 2, while Figure 9(c) was obtained by adding two FO's (Figure 5(a) + Figure 5(b) = Figure 9(a)) previously to the generation of the hologram, using a basic cell. As it is seen, image addition results are independent of the applied method .

However, when the negatives of FO's, shown in Figure 5(a) and (b), are used (see Figure 10(a) and (b)), we can see a difference between both methods. Note the low contrast in Figure 11(a), generated with cell in Figure 2, and in Figure 11(b) with a basic cell, as a consequence of the clear background.

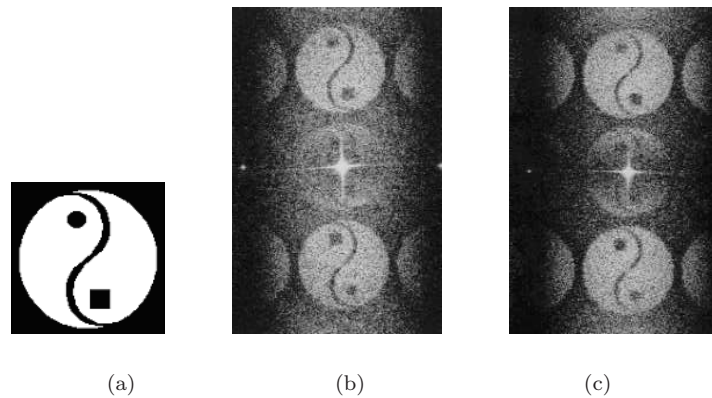


Figure 9. (a) Flat object obtained by direct addition of Figures 4(a) and (b). (b) Image obtained using FO's in Figure 5 and cell in Figure 2. (c) Flat image obtained using flat object in Figure 9(a), and a basic cell.

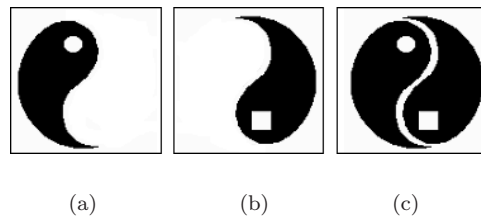


Figure 10. Negatives of FO's in Figure 5.

Analytically these results can be explained as follows. The addition of both FO's in Figure 5(a) and (b) gives as result a flat object in Figure 9(a) whose pixels are valued 0 or 1; while the same procedure with FO's in Figure 10(a) and (b) give a flat object whose pixels are valued 1 or 2, see Figure 10(c). Table I illustrates this concept, where rows 1 - 3 fulfill Figure 9(b) and (c), while rows 2 - 4 fulfill Figure 11(a) and (b).

IV. CONCLUSIONS

It has been shown that it is possible to reconstruct a more complex image from two or three FO's which are codified separately and maintained independent during codification. At this moment three FO's have been recorded.

Therefore, it is evident that, when the amount of information contained in a hologram (by the method proposed) increases, it increases the overlaps between the rectangles in the cell. Studies on this particular subject are now in progress. But note that the finite cell size limits the maximum number of rectangles in the cell.

TABLE I

	X	Y	$X + Y$
Row 1	0	0	0
Row 2	1	0	1
Row 3	0	1	1
Row 4	1	1	2

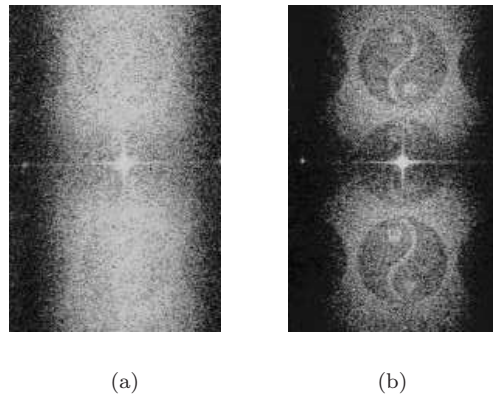


Figure 11. Recuperated images: (a) using FO's in Figure 10(a)-(b) and cell in Figure 2, (note the low contrast); (b) using flat object in Figure 10(c) and a basic cell.

One advantage of the proposed method is that the information can be manipulated to perform simple processing operations as image subtraction and image differentiation in the same direction [7], besides, the images addition as it was showed.

REFERENCES

- [1] Wai-Hon Lee, "Computer-Generated Holograms: Techniques and Applications" Progress in Optics XVI (North-Holland, New York, 1978), pp. 121-232.
- [2] B. R. Brown and A. W. Lohmann, " Complex spatial filtering with binary masks", Appl. Opt. 5, 967-969 (1966).
- [3] A. W. Lohmann and D. P. Paris, "Binary Fraunhofer Holograms Generated by Computer", Appl. Opt. 6, 1739-1748 (1967).
- [4] A. W. Lohmann and Stefan Sinzinger, "Graphic codes for computer holography", Appl. Opt. 34, 3172-3178 (1995).
- [5] D. Mendlovic, "Double-multiplexed computer-generated holograms", Appl. Opt. 35, 3887-3890 (1996).
- [6] R. ChaoHong, Z. Jin and G. WenQi, "Four-channel self-focus computer generated hologram", Appl. Opt. 36, 8844-8847 (1997).
- [7] M. Araiza E., S. Guel S., J. Ojeda C., "Multichannel image storage with image processing capabilities", Opt. Comm. 230, 131-135 (2004).